

# Quasar massive ionized outflows traced by CIV $\lambda 1549$ and [OIII] $\lambda\lambda 4959,5007$

P. Marziani<sup>1,\*</sup>, C. A. Negrete<sup>2,\*</sup>, D. Dultzin<sup>2,\*</sup>, M. L. Martínez-Aldama<sup>3,\*</sup>, A. Del Olmo<sup>3,\*</sup>, M. D'Onofrio<sup>4,\*</sup>, G. M. Stirpe<sup>5,\*</sup>

<sup>1</sup> *INAF, Osservatorio Astronomico di Padova, Italy*

<sup>2</sup> *Instituto de Astronomía, UNAM, Mexico*

<sup>3</sup> *Instituto de Astrofísica de Andalucía (IAA-CSIC), Granada, Spain*

<sup>4</sup> *Università di Padova, Padova, Italia*

<sup>5</sup> *INAF Osservatorio Astronomico di Bologna, Italia*

Correspondence\*:

Paola Marziani

paola.marziani@oapd.inaf.it

## ABSTRACT

The most luminous quasars (with bolometric luminosities are  $\gtrsim 10^{47}$  erg/s) show a high prevalence of CIV  $\lambda 1549$  and [OIII] $\lambda\lambda 4959,5007$  emission line profiles with strong blueshifts. Blueshifts are interpreted as due to Doppler effect and selective obscuration, and indicate outflows occurring over a wide range of spatial scales. We found evidence in favor of the nuclear origin of the outflows diagnosed by [OIII] $\lambda\lambda 4959,5007$ . The ionized gas mass, kinetic power, and mechanical thrust are extremely high, and suggest widespread feedback effects on the host galaxies of very luminous quasars, at cosmic epochs between 2 and 6 Gyr from the Big Bang. In this mini-review we summarize results obtained by our group and reported in several major papers in the last few years with an eye on challenging aspects of quantifying feedback effects in large samples of quasars.

**Keywords:** galaxy evolution – quasars – feedback – outflows – quasars: emission lines – quasars: supermassive black holes

## 1 INTRODUCTION

The broad and narrow high-ionization emission lines (HILs) in the optical and UV spectra of quasars frequently show significant blueshifts with respect to the quasar rest frame (e.g., Gaskell, 1982; Tytler and Fan, 1992; Marziani et al., 1996; Corbin and Boroson, 1996; Zamanov et al., 2002, for some early papers). The interpretation involves the Doppler shift of line radiation due to the emitting gas motion toward the observer, with the part of line emitted by receding gas suppressed by obscuration. In the following we will adhere with this interpretation (for a dissenting view see however Gaskell and Goosmann 2013 who posit that we see light originally emitted by gas falling toward the black hole and backscattered toward us), and consider [OIII] $\lambda 4959,5007$  as representative of narrow high-ionization lines (HILs), and CIV $\lambda 1549$  as a prototypical broad HIL.

## 2 THE QUASAR MAIN SEQUENCE: CONTEXTUALIZING OUTFLOWS AT LOW-TO-MODERATE $L$

The diversity of quasar spectroscopic properties as found in single epoch observations of large samples has been organized along a quasar main sequence (Sulentic et al., 2000a,b; Marziani et al., 2001; Shen and Ho, 2014). Boroson and Green (1992) identified a first eigenvector in their sample of  $\approx 80$  Palomar-Green quasars which is associated with an anticorrelation between FWHM ( $H\beta$ ) and a parameter measuring the prominence of FeII emission (the intensity ratio between the FeII blend at  $\lambda 4570$  and  $H\beta$ ). Along the main sequence defined by this anti-correlation, (Sulentic et al., 2000a) suggested a change in properties in correspondence of FWHM  $H\beta \approx 4000$  km/s, and distinguished two populations: Population A (FWHM  $\lesssim 4000$  km/s) and B (where the B stands for broader than 4000 km/s; e.g., Marziani et al., 2014; Fraix-Burnet et al., 2017, for reviews; Table 1 of Fraix-Burnet et al. 2017 summarized parameter systematic differences between the two populations). Population A and B have been associated with high and low accretion, respectively.

The CIV $\lambda 1549$  large blueshifts (above 1000 km/s) are a Population A phenomenon, likely associated with a disk wind (see Figure 7 of Sulentic and Marziani 2015). Population A sources, at low  $z$  ( $\lesssim 1$ ), encompass relatively low black hole mass quasars ( $\sim 10^7 - 10^8 M_\odot$ ) radiating at a relatively high Eddington ratio ( $\gtrsim 0.1 - 0.2$ ). In many ways Pop. A sources can be considered as an extension of Narrow Line Seyfert 1 (NLSy1) with moderate or strong FeII emission: the limit FWHM  $\approx 4000$  km/s (valid at bolometric luminosity  $\log L \lesssim 47$  [erg s $^{-1}$ ]) allows one to include sources with the same Balmer line profiles and intensity ratios as observed in NLSy1s. This is not to imply that Pop. B sources (with FWHM  $H\beta \gtrsim 4000$  km/s) do not show evidence of outflows. Evidence of outflow is, for example, overwhelming in the prototypical Pop. B source NGC 5548 (Kaastra et al., 2014). The latest developments suggest that outflows are ubiquitous, also in forms that may not provide striking optical/UV spectral phenomenologies (e.g., Tombesi et al., 2015; Harrison et al., 2014). Only, outflows are more difficult to trace in Population B single-epoch spectra, as the CIV integrated line profiles are relatively symmetric. In both Pop. A and B, the CIV $\lambda 1549$  line profile can be represented as a scaled  $H\beta$  profile plus an excess of blueshifted emission: the two components are assumed to be representative of a “virialized” low-ionization broad line region (producing a fairly symmetric and unshifted line) plus an outflow/wind component with different physical conditions. In Pop. B, CIV $\lambda 1549$  shows only a small blueshifted excess if compared to  $H\beta$ .

Similarly, large blueshifts of [OIII] $\lambda\lambda 4959,5007$  above 250 km/s are rare in  $z$  samples (they are real statistical outliers, called “blue outliers” [BOs] by Zamanov et al. 2002) and have been preferentially found among Population A sources (e.g., Zamanov et al., 2002; Xu et al., 2012; Zhang et al., 2013; Cracco et al., 2016). Sulentic and Marziani (2015) show the distribution of [OIII] $\lambda\lambda 4959,5007$  peak shifts for the spectral types defined along the Eigenvector 1 sequence: the prevalence of [OIII] $\lambda\lambda 4959,5007$  large blueshifts increases in Pop. A and reaches a maximum in extreme sources with FeII $\lambda 4570/H\beta \gtrsim 1$  (Figure 5 of Sulentic and Marziani 2015; Negrete et al. 2017, in preparation). Blueshifts of [OIII] $\lambda\lambda 4959,5007$  trace larger scale outflows than CIV $\lambda 1549$ , outside of the broad line region (BLR).

## 3 THE SCENARIO AT HIGH $L$ , AND INTERMEDIATE- $z$

A recent result is that the prevalence of large blueshifts in both CIV $\lambda 1549$  and [OIII] $\lambda 4959,5007$  quasars is much higher at high  $L$  in intermediate- $z$  samples ( $1 \lesssim z \lesssim 2.5$ , Marziani et al., 2016a; Coatman et al., 2016; Zakamska et al., 2016; Vietri, 2017; Bischetti et al., 2017, M16). Blueshifts of CIV $\lambda 1549$  reach several thousands km/s in Pop. A. BOs become much more frequent in the high  $z$  and  $L$  samples. The [OIII]

shift and FWHM distributions at high- $L$  are remarkably different from those of low- $z$ , low  $L$  samples. Figure 1 shows an example of a luminous Pop. A source in the sample of Sulentic et al. (2017): the left panel shows, overlaid to the continuum-subtracted spectrum, a decomposition of the CIV $\lambda$ 1549 profile into an unshifted and symmetric component (thick black line) and a blue shifted component (blue line). Without involving any profile decomposition (the caveats of the technique are discussed in Negrete et al. 2014), it is easy to see that about 80% of the line flux is emitted short-wards of the rest wavelength. At the same time, the H $\beta$  remains symmetric. Fig. 1 (rightmost panel) shows an enlargement of the [OIII] $\lambda$ 4959,5007 profile: the FWHM  $\approx$  3600 km/s is extremely broad by [OIII] $\lambda$ 5007 standards (at low- $z$ , [OIII] $\lambda$ 5007 FWHM is  $\lesssim$  1000 km/s). The profile appears boxy, and fully displaced to the blue.

Figure 1 represents the diagnostic provided by single epoch observations for quasars at intermediate-to-high  $z$  (1 – 5), with CIV $\lambda$ 1549 covered by optical spectrometers and [OIII] $\lambda$ 4959,5007 requiring near-IR spectroscopic observations. The latter have become possible for relatively faint quasars only in recent times, with the advent of second generation IR spectrometers mounted at the foci of large aperture telescopes; two major examples are XSHOOTER at VLT and LUCI at LBT. Near IR observations provide a reliable estimate of the quasar systemic redshift if the narrow component of H $\beta$  or the [OII] $\lambda$ 3727 can be effectively measured. If these lines are detected above noise, then a good precision in the rest frame can be achieved, and the uncertainty is typically  $\delta z \lesssim 3 \cdot 10^{-4}$ . An accurate knowledge of the rest frame is not an end in itself, since an important physical parameter such as the outflow kinetic power depends on the third power of the outflow velocity  $v_o$ . The availability of such observations should increase dramatically in the next few years, providing useful data (even with lack of real spatial resolution) for a better understanding of the outflow prevalence and power as a function of luminosity and cosmic epoch. At low- $z$ , partial spatial resolution of the [OIII] $\lambda$ 4959,5007 emitting regions is currently obtained (and will be more frequently obtained in the coming years) with the use of integral-field unit spectrographs with adaptive optics (e.g., Cresci et al., 2015). Observations of CIV $\lambda$ 1549 are and will remain challenging for sources at  $z \lesssim 1.2$  i.e., for all the low- $z$  quasar population.

### 3.1 The nuclear nature of the outflow

CIV $\lambda$ 1549 emission is expected to originate within a few hundred gravitational radii from the central black hole even in luminous quasars (Kaspi et al., 2007). Reverberation mapping studies indicate that the CIV emitting region scaling law with luminosity is a power-law with exponent 0.5 – 0.7 (results by Shai Kaspi in this research topic). The nuclear nature of the CIV $\lambda$ 1549 outflow is not in question.

The [OIII] $\lambda$ 4959,5007 prominence is affected by the “Baldwin effect” (Zhang et al., 2011), which is perhaps the main luminosity effect affecting all HILs (Dietrich et al., 2002). The observations of samples covering a wide range in luminosity ( $43 \lesssim \log L \lesssim 48.5$  [erg/s]) confirm the [OIII] Baldwin effect:  $W \propto L_{5100}^{-0.26 \pm 0.03}$  (M16), steeper than the “classical” CIV Baldwin effect. However, a most intriguing result is that sources with large [OIII] blueshifts (the “blue outliers” of Zamanov et al. 2002) do not follow any Baldwin effect:  $W \propto L_{5100}^{0.050 \pm 0.066}$ , as shown in Figure 4 of M16. In other words, for sources with large blueshifts, the line luminosity is proportional to the continuum luminosity. The simplest explanation is that [OIII] $\lambda$ 4959,5007 emission is due to photoionization by the nuclear continuum.

Fig. 2 shows a sketch explaining this result. At low- $L$ , emission of [OIII] $\lambda$ 4959,5007 shows a spiky core and a prominent blueward asymmetry, especially in Pop. B sources. If the line profile is interpreted as made of a core component and a blue shifted semi broad component, then the latter component is not dominating at low- $z$  and low- $L$  unless we are considering a system radiating at high- Eddington ratio: these sources show *only* the semi broad component. At high- $L$  the semi-broad component becomes so luminous

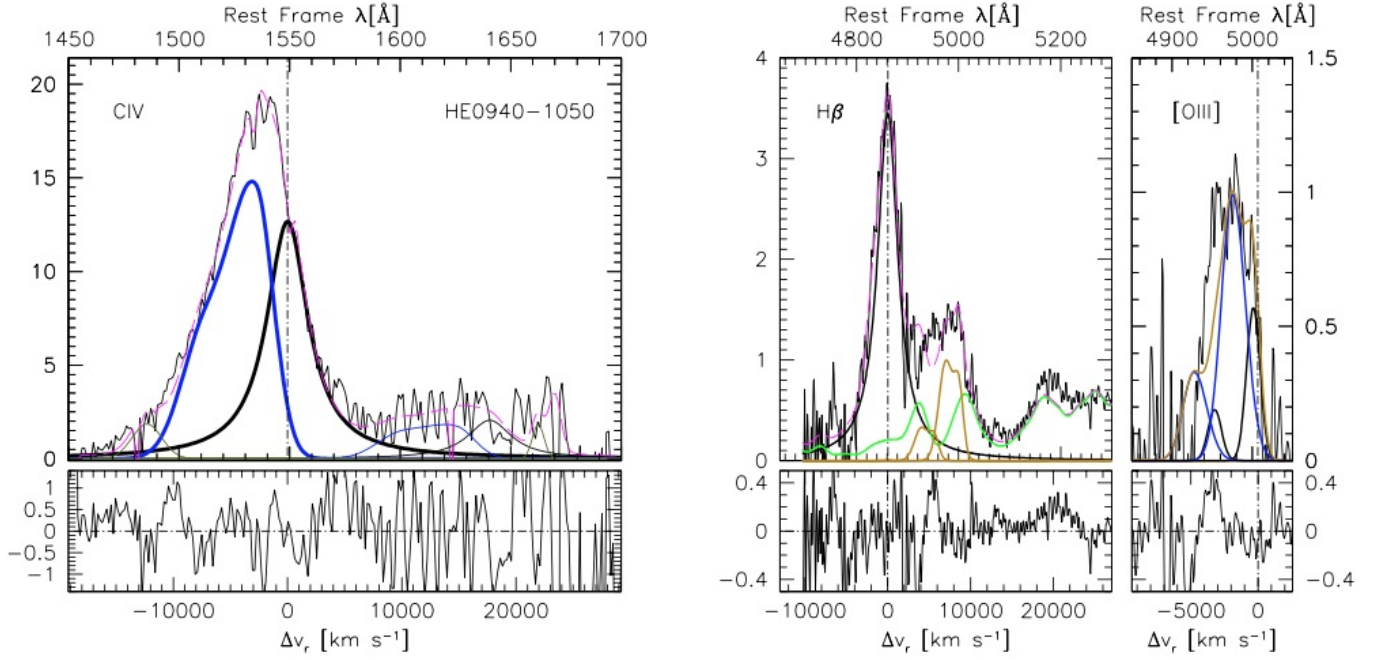


**Figure 1.** Left panel: CIV  $\lambda 1549$  emission after continuum subtraction. A scaled  $H\beta$  profile is superimposed (adapted from Sulentic et al. 2017). Right panel:  $H\beta$  spectral range. The green line shows the adopted FeII template. The full profiles of [OIII]  $\lambda\lambda 4959, 5007$  are shown in orange. The thick black lines identify a symmetric unshifted emission that is dominating  $H\beta$  and still contributing to CIV  $\lambda 1549$ . The thick blue lines trace the excess emission once the symmetric component is subtracted. The thin lines in the CIV panel show the interpretation of the HeII  $\lambda 1640$  profile assuming a symmetric and a blue shifted component, as for CIV. The rightmost panel provides an enlargement on the [OIII]  $\lambda\lambda 4959, 5007$ , semi-broad, boxy and blue-shifted profile (not a unique case at high  $L$ : e.g., Cano-Díaz et al. 2012). The [OIII] profile is modeled as the sum of a moderately blueshifted core component (black line) and of a semi-broad component, blue-shifted by  $\approx -2500$  km/s (blue line). The scale is  $10^{-15}$  erg s $^{-1}$  cm $^{-2}$  Å $^{-1}$  in the rest frame, as applied by Sulentic et al. (2017).

**Table 1.** Outflow physical parameters derived for CIV and [OIII]: mass of ionized gas, mass outflow rate, thrust and kinetic power

Parameter	Units	CIV	[OIII]
$M^{\text{ion}}$	$M_{\odot}$	$1.9 \cdot 10^3 L_{45} \left(\frac{Z}{5Z_{\odot}}\right)^{-1} n_9^{-1}$	$1 \cdot 10^7 L_{44} \left(\frac{Z}{5Z_{\odot}}\right)^{-1} n_3^{-1}$
$\dot{M}^{\text{ion}}$	$M_{\odot} \text{ yr}^{-1}$	$30 L_{45} v_{o,5000} r_{1\text{pc}}^{-1} \left(\frac{Z}{5Z_{\odot}}\right)^{-1} n_9^{-1}$	$30 L_{44} v_{o,1000} r_{1\text{kpc}}^{-1} \left(\frac{Z}{5Z_{\odot}}\right)^{-1} n_3^{-1}$
$\dot{M}^{\text{ion}} k v_o$	$\text{g cm s}^{-2}$	$1 \cdot 10^{36} L_{45} k v_{o,5000}^2 r_{1\text{pc}}^{-1} \left(\frac{Z}{5Z_{\odot}}\right)^{-1} n_9^{-1}$	$1.9 \cdot 10^{35} L_{44} k v_{o,1000}^2 r_{1\text{kpc}}^{-1} \left(\frac{Z}{5Z_{\odot}}\right)^{-1} n_3^{-1}$
$\dot{\epsilon}$	$\text{erg s}^{-1}$	$2.4 \cdot 10^{44} L_{45} k^2 v_{o,5000}^3 r_{1\text{pc}}^{-1} \left(\frac{Z}{5Z_{\odot}}\right)^{-1} n_9^{-1}$	$9.6 \cdot 10^{42} L_{44} k^2 v_{o,1000}^3 r_{1\text{kpc}}^{-1} \left(\frac{Z}{5Z_{\odot}}\right)^{-1} n_3^{-1}$

to overwhelm the core component whose luminosity is expected to be upper-bound by the physical size and gas content of the host galaxy (Netzer et al., 2004).

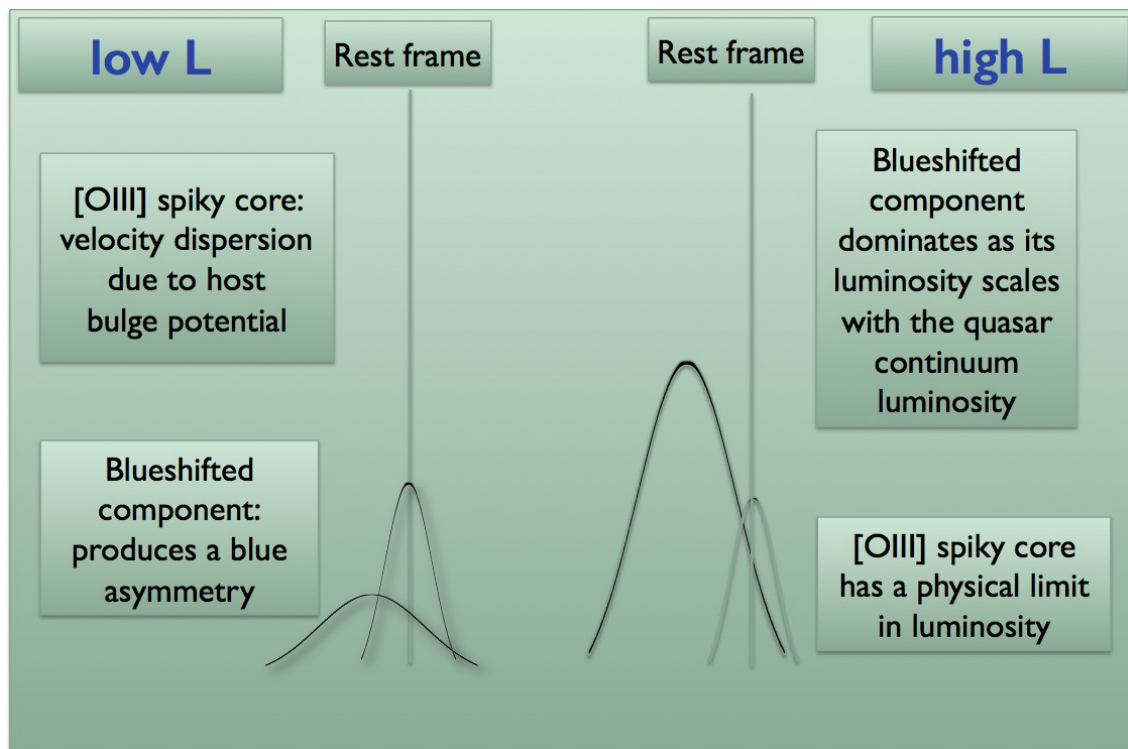


**Figure 2.** The high prevalence of large [OIII] $\lambda\lambda 4959,5007$  blueshift at high  $L$  explained as a luminosity effect. The luminosity of the blue shifted component grows with the nuclear continuum luminosity, dominating the total [OIII] emission in very luminous quasars. Fig. 6 of M16 shows the same effect in terms of EW: the EW of the core component is lower in very luminous sources because of the strong nuclear continuum, while the EW of the blue shifted component remains constant.

#### 4 ESTIMATES OF OUTFLOW DYNAMICAL PARAMETERS AND CONSIDERATIONS ON THEIR RELIABILITY

Computing the kinetic power and the thrust from single-epoch spectra is possible under several caveats and assumptions. Here we briefly recall a simplified way to estimate the mass of ionized gas, the mass outflow rate, the thrust, and the kinetic power of the outflow for collisional excited lines in photoionized gases (Cano-Díaz et al., 2012). The formation of these authors allows to write the outflow parameters in a form independent from the covering and filling factor, provided that all emitting gas has the same density. The simplified approach is well-suited to elucidate the role of the most relevant outflow parameters in the computation of the thrust and kinetic power. We will then consider the specific assumptions needed to apply the following relation to [OIII] and CIV measures from single epoch spectra.

The luminosity of any collisionally-excited line<sup>1</sup> is given by  $L(\text{line}) = \int_V j_{\text{line}} f_{\text{f}} dV$ , where  $j_{\text{line}}$  is the line emissivity per unit volume, and can be written as:  $j_{\text{line}} = h\nu q_{\text{lu}} n_e n_l$ , where  $n_e$  the electron density, and  $n_l$  the number density of ions at the lower level of the transition. The collisional excitation rate at electron temperature  $T$  is  $q_{\text{lu}} = \frac{\beta}{\sqrt{T}} \frac{\Upsilon_{\text{lu}}}{g_l} \exp\left(-\frac{\epsilon_{\text{lu}}}{kT}\right)$ , where  $g_l$  is the statistical weight of the lower level, and  $\Upsilon_{\text{lu}}$  is the effective collision strength. The line luminosity can be connected to the mass of ionized gas

<sup>1</sup> While the ionic stages of  $\text{C}^{3+}$  and  $\text{O}^{2+}$  are due to photoionization, the CIV and [OIII] lines are produced via collisional excitation which is dominant over recombination, as shown in detail for [OIII] in Pradhan and Nahar (2015), §12.4.

since  $M_{\text{out}}^{\text{ion}} \propto L_{\text{line}} \left(\frac{Z}{Z_{\odot}}\right)^{-1} n^{-1}$ . Up to this point the main assumptions are: (1) constant density; (2) all emitting gas being in the ionization stage that is producing the line; (3) well defined chemical abundances.

The mass outflow rate at a distance  $r$  can be written as, if the flow is confined to a solid angle of  $\Omega$  of volume  $\frac{4}{3}\pi r^3 \frac{\Omega}{4\pi}$ :  $\dot{M}_0^{\text{ion}} = \rho \Omega r^2 v_0 = \frac{M_0^{\text{ion}}}{V} \Omega r^2 v_0 \propto L v_0 r^{-1}$ . This requires the knowledge of (4) a typical emitting region radius, and (5) the outflow velocity  $v_0$ . Assuming a single  $r$  value is already a strong simplification, especially for [OIII]. If the line emitting gas is still being accelerated (as in the CIV case), and the terminal velocity is  $v_{\text{term}} = k v_0$ , then the thrust should be  $\propto \dot{M} k v_0$  and the kinetic power of the outflow  $\dot{\epsilon} \sim \frac{1}{2} \dot{M}^{\text{ion}} k^2 v_0^2 \propto L_{\text{line}} k^2 v_0^3 r^{-1}$ . A value of  $k=1$  can be assumed for [OIII] (as explained in §4.2). The parameters of Table 1 can be all written in the form  $\propto L_{\text{line}} r^{-1} n^{-1} (Z/Z_{\odot})^{-1} v_0^n$ , with  $0 \leq n \leq 3$ . The BLR gas exhibits highly super-solar chemical composition (Nagao et al., 2006; Shin et al., 2013), so that assuming  $Z = 5Z_{\odot}$  is a reasonable choice for both [OIII] and CIV outflow, if the [OIII] emission is ascribed to a nuclear outflow. Finally, to be consistent with the idea of a *bipolar* outflow, all the quantities in Table 1 have been multiplied by a factor 2.

It is interesting to make some considerations on the most likely values of the outflow parameters in very luminous quasars, and somehow constrain their upper limits. The considerations below are focused on very luminous quasars such as the ones studied by the WISSH project and by Sulentic et al. (2017) and M16. We will consider here the 14 Pop. A objects of the ‘‘HE’’ sample of M16 and Marziani et al. (2016a) with  $47.5 \lesssim \log L \lesssim 48.5 \text{ erg s}^{-1}$ . The relations of Table 1 are scaled to values typical of the HE sample. In the redshift range  $1 \lesssim z \lesssim 2.5$  where the population of most luminous quasars peaks, the angular distance is not increasing anymore with redshift (Hogg, 1999), implying a fairly constant scale around 8 Kpc/arcsec. For standard ground based observations, with a slit width of 0.5 – 1 arcsec, all emission from CIV is collected (obviously) and most or at least a significant fraction of [OIII] should be collected as well, although not necessarily all of it: [OIII] emission may extend to the outer boundaries of optical galaxies and even beyond (see, for instance, the impressive case of NGC 5252, Tadhunter and Tsvetanov 1989).

#### 4.1 CIV

Estimating  $L_{\text{line}}$  associated with unbound gas is not trivial, since the CIV emitting gas is probably still being accelerated by strong radiation forces within the BLR. As a lower limit, one can consider the fraction of the line that is already above a projected escape velocity. A more proper approach may be to consider that the gas is outflowing (i.e., the blue shifted component of Fig. 1), and use a model in which gas cloud motions are accelerated under the effects of gravitation and radiation force (for example Netzer and Marziani 2010). In this case the  $v$  entering the equations of the thrust and the kinetic power should be the terminal velocity  $v_{\text{term}}$ , larger than the outflow velocity  $v$  at  $r_{\text{CIV}}$ . The CIV emitting region radius can be computed from the radius-luminosity relation derived for CIV,  $r_{\text{CIV}} \propto L^b$ , with  $b \approx 0.5 - 0.7$  (Kaspi et al., 2007, see also contribution in the same research topic). While the density of the low-ionization part of the BLR is fairly well constrained (Negrete et al., 2012; Martínez-Aldama et al., 2015), the density of the outflowing component is not, although we can assume  $8 \leq \log n \leq 10 \text{ [cm}^{-3}\text{]}$ ,  $0.2 \leq L_{\text{line}}/L_{\text{line,tot}} \leq 1$ . The thrust and the kinetic power may be larger than the values reported in Table 1 by a factor 10 and 100 respectively if radiative acceleration drives a wind with  $k \approx 10$  which may be the case for high Eddington ratio ( $\gtrsim 0.7$ , following Netzer and Marziani 2010).

#### 4.2 [OIII]

For reasonable values of  $r$ , almost all of the blue shifted [OIII] emission should have escaped from the BH gravitational pull ( $k = 1$ ). The full value of  $L_{\text{line}}$  could be taken as a first guess of the outflowing

gas luminosity. It is also reasonable to assume that the gas density is between the [OIII] critical density  $\log n \sim 5.5$  [ $\text{cm}^{-3}$ ] and the typical density of outer narrow line regions,  $\log n \sim 3$  [ $\text{cm}^{-3}$ ]. The distance  $r$  remains a critical parameter in the absence of spatially resolved information. The ISAAC observations of the HE sample (M16) were carried out with a slit width of 0.6 arcsec centered on the quasar: this implies that emission within  $\approx 2.4$  kpc was collected. Imposing mass conservation ( $\dot{M}_{[\text{OIII}]} \approx \dot{M}_{\text{CIV}}$ , and [OIII] emission at critical density implies  $r_{[\text{OIII}]} \sim [5 \cdot 10^9 / 10^5]^{\frac{1}{2}} \sim 10^{2.35} \sim 2 \cdot 10^2$  pc, if  $v_{[\text{OIII}]} / v_{\text{CIV}} \approx 5$ , and  $r_{\text{CIV}} \approx 1$  pc. An alternative assumption is motivated by previous results on the low- $z$  blue outliers: it was possible to model both CIV and [OIII] with the same velocity field, assuming that the two lines were emitted with a velocity a constant factor 1.5 the local virial velocity i.e., slightly above the local escape velocity (Zamanov et al., 2002, cf. Komossa et al. 2008). Then  $v_{[\text{OIII}]} / v_{\text{CIV}} = \sqrt{r_{\text{CIV}} / r_{[\text{OIII}]}}$ , if the factor remains the same for the two lines. We derive  $r_{[\text{OIII}]} \approx 25$  pc. This line of reasoning clearly emphasizes the necessity of obtaining spatially-resolved [OIII] data with density diagnostics, and of tracking the velocity field as close as possible to the nucleus in prototypical cases that could help constrain observations lacking spatial resolution.

### 4.3 Relation to luminosity and radiation thrust

The average luminosity of the Population A HE sample sources is  $\approx 10^{47.8}$  erg/s. The average peak velocity shift of the Pop. A CIV blueshifted component is  $\approx -3000$  km/s. Typical  $r_{\text{CIV}}$  are around 1pc, and the typical CIV luminosity is  $10^{45}$  erg/s. Even assuming  $k = 10$ ,  $v_o \approx 3000$  km/s, the  $\epsilon$  value is several orders of magnitude below the bolometric luminosity:  $\log \epsilon \approx \log L - 2.4$ , a factor ten lower than the value of 5% efficiency needed for a structural and dynamical effect on the host galaxy (e.g., King and Pounds, 2015). This limit might however be reached if the gas density is a factor  $\approx 10$  lower than assumed. Similar considerations apply to [OIII]: if the outflow is more compact than assumed in Table 1, then an increase by a factor 10 – 50 is possible. However, with the values of Tab. 1 the estimates for  $\log \epsilon$  for [OIII] are four orders of magnitude below  $0.05L$ .

The mechanical thrust values  $\dot{M}v_o$  are also lower than the radiation thrust  $L/c \sim 10^{37.3}$  g cm s $^{-2}$ . Again,  $\dot{M}v_o$  may reach values of the same order or in excess by a factor of 20 of the radiation thrust (Zubovas and King, 2012) if  $n$  is lower in the case of CIV and  $r$  for [OIII] is  $\ll 1$  Kpc. A similar scenario involving  $\dot{M}v_o$  and  $\epsilon$  too low at face values to explain the black hole – bulge mass relation was depicted by Carniani et al. (2015). Accepted at face values, these estimates suggest that, even in these very luminous quasars, the mechanical feedback estimated from mildly ionized gas may not be sufficient to reach the effect necessary for an evolutionary feedback on the host galaxy, unless the outflow parameter are stretched to the limit of plausible values. Even if the required conditions are met, the observations do not exclude an important role of the active nucleus radiation force in driving the outflow. In addition, the estimates sample only one component of the nuclear outflow: the mildly ionized one which is, especially for the BLR, associated to a relatively small amount of matter. High ionization plasma, atomic and molecular gases are not considered, although even in the local Universe we have a spectacular example of massive molecular outflow, Mark 231 (e.g., Feruglio et al., 2015).

## 5 CONCLUSION

Evidence of HIL blueshifts are ubiquitous, and at high luminosity they become impressive involving very large shifts in broad and narrow HILs. The mass outflow rates indicated by both [OIII] and CIV are extremely high, only somewhat lower than the accretion mass influx needed to sustain the observed luminosity for modest radiative efficiency ( $\sim 100 M_{\odot} \text{ yr}^{-1}$  at efficiency 0.1). Even in the most luminous

quasars, it is not obvious whether powerful outflows can have the ability to disrupt the host galaxy gas. However, it is likely that [OIII] and CIV trace only a part of the mass outflow. Accounting for multiphase outflows will be one of the major challenges of present and future observational and theoretical studies.

## FUNDING

A.d.O., and M.L.M.A. acknowledge financial support from the Spanish Ministry for Economy and Competitiveness through grants AYA2013-42227-P and AYA2016-76682-C3-1-P. J. P. acknowledges financial support from the Spanish Ministry for Economy and Competitiveness through grants AYA2013-40609-P and AYA2016-76682-C3-3-P. D. D. and A. N. acknowledge support from grants PAPIIT108716, UNAM, and CONACyT221398.

## REFERENCES

- Bischetti, M., Piconcelli, E., Vietri, G., Bongiorno, A., Fiore, F., Sani, E., et al. (2017). The WISSH quasars project. I. Powerful ionised outflows in hyper-luminous quasars. *Astron. Astroph.* 598, A122. doi:10.1051/0004-6361/201629301
- Boroson, T. A. and Green, R. F. (1992). The emission-line properties of low-redshift quasi-stellar objects. *ApJS* 80, 109–135. doi:10.1086/191661
- Cano-Díaz, M., Maiolino, R., Marconi, A., Netzer, H., Shemmer, O., and Cresci, G. (2012). Observational evidence of quasar feedback quenching star formation at high redshift. *Astron. Astroph.* 537, L8. doi:10.1051/0004-6361/201118358
- Carniani, S., Marconi, A., Maiolino, R., Balmaverde, B., Brusa, M., Cano-Díaz, M., et al. (2015). Ionised outflows in  $z \sim 2.4$  quasar host galaxies. *Astron. Astroph.* 580, A102. doi:10.1051/0004-6361/201526557
- Coatman, L., Hewett, P. C., Banerji, M., and Richards, G. T. (2016). C iv emission-line properties and systematic trends in quasar black hole mass estimates. *Mon. Not. R. Astron. Soc.* 461, 647–665. doi:10.1093/mnras/stw1360
- Corbin, M. R. and Boroson, T. A. (1996). Combined Ultraviolet and Optical Spectra of 48 Low-Redshift QSOs and the Relation of the Continuum and Emission-Line Properties. *Astroph. J. Suppl. Ser.* 107, 69. doi:10.1086/192355
- Cracco, V., Ciroi, S., Berton, M., Di Mille, F., Foschini, L., La Mura, G., et al. (2016). A spectroscopic analysis of a sample of narrow-line Seyfert 1 galaxies selected from the Sloan Digital Sky Survey. *Mon. Not. R. Astron. Soc.* 462, 1256–1280. doi:10.1093/mnras/stw1689
- Cresci, G., Marconi, A., Zibetti, S., Risaliti, G., Carniani, S., Mannucci, F., et al. (2015). The MAGNUM survey: positive feedback in the nuclear region of NGC 5643 suggested by MUSE. *Astron. Astroph.* 582, A63. doi:10.1051/0004-6361/201526581
- Dietrich, M., Hamann, F., Shields, J. C., Constantin, A., Vestergaard, M., Chaffee, F., et al. (2002). Continuum and Emission-Line Strength Relations for a Large Active Galactic Nuclei Sample. *Astroph. J.* 581, 912–924. doi:10.1086/344410
- Feruglio, C., Fiore, F., Carniani, S., Piconcelli, E., Zappacosta, L., Bongiorno, A., et al. (2015). The multi-phase winds of Markarian 231: from the hot, nuclear, ultra-fast wind to the galaxy-scale, molecular outflow. *Astron. Astroph.* 583, A99. doi:10.1051/0004-6361/201526020
- Fraix-Burnet, D., Marziani, P., D’Onofrio, M., and Dultzin, D. (2017). The phylogeny of quasars and the ontogeny of their central black holes. *Frontiers in Astronomy and Space Sciences* 4, 1. doi:10.3389/fspas.2017.00001

- Gaskell, C. M. (1982). A redshift difference between high and low ionization emission-line regions in QSOs - Evidence for radial motions. *ApJ* 263, 79–86. doi:10.1086/160481
- Gaskell, C. M. and Goosmann, R. W. (2013). Line Shifts, Broad-line Region Inflow, and the Feeding of Active Galactic Nuclei. *Astroph. J.* 769, 30. doi:10.1088/0004-637X/769/1/30
- Harrison, C. M., Alexander, D. M., Mullaney, J. R., and Swinbank, A. M. (2014). Kiloparsec-scale outflows are prevalent among luminous AGN: outflows and feedback in the context of the overall AGN population. *Mon. Not. R. Astron. Soc.* 441, 3306–3347. doi:10.1093/mnras/stu515
- Hogg, D. W. (1999). Distance measures in cosmology. *ArXiv Astrophysics e-prints* astro-ph/9905116
- Kaastra, J. S., Kriss, G. A., Cappi, M., Mehdipour, M., Petrucci, P.-O., Steenbrugge, K. C., et al. (2014). A fast and long-lived outflow from the supermassive black hole in NGC 5548. *Science* 345, 64–68. doi:10.1126/science.1253787
- Kaspi, S., Brandt, W. N., Maoz, D., Netzer, H., Schneider, D. P., and Shemmer, O. (2007). Reverberation Mapping of High-Luminosity Quasars: First Results. *Astroph. J.* 659, 997–1007. doi:10.1086/512094
- King, A. and Pounds, K. (2015). Powerful Outflows and Feedback from Active Galactic Nuclei. *Ann. Rev. Astron. Astroph.* 53, 115–154. doi:10.1146/annurev-astro-082214-122316
- Komossa, S., Xu, D., Zhou, H., Storchi-Bergmann, T., and Binette, L. (2008). On the Nature of Seyfert Galaxies with High [O III]  $\lambda$ 5007 Blueshifts. *Astroph. J.* 680, 926–938. doi:10.1086/587932
- Martínez-Aldama, M. L., Dultzin, D., Marziani, P., Sulentic, J. W., Bressan, A., Chen, Y., et al. (2015). O I and Ca II Observations in Intermediate Redshift Quasars. *ApJS* 217, 3. doi:10.1088/0067-0049/217/1/3
- Marziani, P., Martínez Carballo, M. A., Sulentic, J. W., Del Olmo, A., Stirpe, G. M., and Dultzin, D. (2016a). The most powerful quasar outflows as revealed by the Civ  $\lambda$ 1549 resonance line. *Astroph. Space Sci.* 361, 29. doi:10.1007/s10509-015-2611-1
- Marziani, P., Sulentic, J. W., Dultzin-Hacyan, D., Calvani, M., and Moles, M. (1996). Comparative Analysis of the High- and Low-Ionization Lines in the Broad-Line Region of Active Galactic Nuclei. *ApJS* 104, 37–+. doi:10.1086/192291
- Marziani, P., Sulentic, J. W., Negrete, C. A., Dultzin, D., D’Onofrio, M., Del Olmo, A., et al. (2014). Low- and high- $z$  highly accreting quasars in the 4D Eigenvector 1 context. *The Astronomical Review* 9, 6–25
- Marziani, P., Sulentic, J. W., Stirpe, G. M., Dultzin, D., Del Olmo, A., and Martínez-Carballo, M. A. (2016b). Blue outliers among intermediate redshift quasars. *Astroph. Space Sci.* 361, 3. doi:10.1007/s10509-015-2590-2
- Marziani, P., Sulentic, J. W., Zwitter, T., Dultzin-Hacyan, D., and Calvani, M. (2001). Searching for the Physical Drivers of the Eigenvector 1 Correlation Space. *ApJ* 558, 553–560. doi:10.1086/322286
- Nagao, T., Marconi, A., and Maiolino, R. (2006). The evolution of the broad-line region among SDSS quasars. *A&Ap* 447, 157–172. doi:10.1051/0004-6361:20054024
- Negrete, A., Dultzin, D., Marziani, P., and Sulentic, J. (2012). BLR Physical Conditions in Extreme Population A Quasars: a Method to Estimate Central Black Hole Mass at High Redshift. *ApJ* 757, 62
- Negrete, C. A., Dultzin, D., Marziani, P., and Sulentic, J. W. (2014). A New Method to Obtain the Broad Line Region Size of High Redshift Quasars. *Astroph. J.* 794, 95. doi:10.1088/0004-637X/794/1/95
- Netzer, H. and Marziani, P. (2010). The Effect of Radiation Pressure on Emission-line Profiles and Black Hole Mass Determination in Active Galactic Nuclei. *Astroph. J.* 724, 318–328. doi:10.1088/0004-637X/724/1/318
- Netzer, H., Shemmer, O., Maiolino, R., Oliva, E., Croom, S., Corbett, E., et al. (2004). Near-Infrared Spectroscopy of High-Redshift Active Galactic Nuclei. II. Disappearing Narrow-Line Regions and the Role of Accretion. *Astroph. J.* 614, 558–567. doi:10.1086/423608

- Pradhan, A. K. and Nahar, S. N. (2015). *Atomic Astrophysics and Spectroscopy* (Cambridge University Press)
- Shen, Y. and Ho, L. C. (2014). The diversity of quasars unified by accretion and orientation. *Nature* 513, 210–213. doi:10.1038/nature13712
- Shin, J., Woo, J.-H., Nagao, T., and Kim, S. C. (2013). The Chemical Properties of Low-redshift QSOs. *Astroph. J.* 763, 58. doi:10.1088/0004-637X/763/1/58
- Sulentic, J. and Marziani, P. (2015). Quasars in the 4D Eigenvector 1 Context: a stroll down memory lane. *Frontiers in Astronomy and Space Sciences* 2, 6. doi:10.3389/fspas.2015.00006
- Sulentic, J. W., del Olmo, A., Marziani, P., Martínez-Carballo, M. A., D’Onofrio, M., Dultzin, D., et al. (2017). What does Civ $\{\lambda\}$ 1549 tell us about the physical driver of the Eigenvector Quasar Sequence? *ArXiv e-prints*
- Sulentic, J. W., Marziani, P., and Dultzin-Hacyan, D. (2000a). Phenomenology of Broad Emission Lines in Active Galactic Nuclei. *ARA&A* 38, 521–571. doi:10.1146/annurev.astro.38.1.521
- Sulentic, J. W., Marziani, P., Zwitter, T., Dultzin-Hacyan, D., and Calvani, M. (2000b). The Demise of the Classical Broad-Line Region in the Luminous Quasar PG 1416-129. *ApJL* 545, L15–L18. doi:10.1086/317330
- Tadhunter, C. and Tsvetanov, Z. (1989). Anisotropic ionizing radiation in NGC5252. *Nature* 341, 422–424. doi:10.1038/341422a0
- Tombesi, F., Melendez, M., Veilleux, S., Reeves, J. N., Gonzalez-Alfonso, E., and Reynolds, C. S. (2015). Wind from the black-hole accretion disk driving a molecular outflow in an active galaxy. *ArXiv e-prints*
- Tytler, D. and Fan, X.-M. (1992). Systematic QSO emission-line velocity shifts and new unbiased redshifts. *ApJS* 79, 1–36. doi:10.1086/19\ -16\ -42
- Vietri, G. (2017). The LBT/WISSH quasar survey: revealing powerful winds in the most luminous AGN. In *American Astronomical Society Meeting Abstracts*. vol. 229 of *American Astronomical Society Meeting Abstracts*, 302.06
- Xu, D., Komossa, S., Zhou, H., Lu, H., Li, C., Grupe, D., et al. (2012). Correlation Analysis of a Large Sample of Narrow-line Seyfert 1 Galaxies: Linking Central Engine and Host Properties. *Astron. J.* 143, 83. doi:10.1088/0004-6256/143/4/83
- Zakamska, N. L., Hamann, F., Pâris, I., Brandt, W. N., Greene, J. E., Strauss, M. A., et al. (2016). Discovery of extreme [O III]  $\lambda$ 5007 Å outflows in high-redshift red quasars. *Mon. Not. R. Astron. Soc.* 459, 3144–3160. doi:10.1093/mnras/stw718
- Zamanov, R., Marziani, P., Sulentic, J. W., Calvani, M., Dultzin-Hacyan, D., and Bachev, R. (2002). Kinematic Linkage between the Broad- and Narrow-Line-emitting Gas in Active Galactic Nuclei. *ApJL* 576, L9–L13. doi:10.1086/342783
- Zhang, K., Dong, X.-B., Wang, T.-G., and Gaskell, C. M. (2011). The Blueshifting and Baldwin Effects for the [O III]  $\lambda$ 5007 Emission Line in Type 1 Active Galactic Nuclei. *Astroph. J.* 737, 71. doi:10.1088/0004-637X/737/2/71
- Zhang, K., Wang, T.-G., Gaskell, C. M., and Dong, X.-B. (2013). The Baldwin Effect in the Narrow Emission Lines of Active Galactic Nuclei. *Astroph. J.* 762, 51. doi:10.1088/0004-637X/762/1/51
- Zubovas, K. and King, A. (2012). Clearing Out a Galaxy. *Astroph. J. Lett.* 745, L34. doi:10.1088/2041-8205/745/2/L34